



**HAL**  
open science

## Two-photon Dye-Based Fluorogenic Organic Nanoparticles as Intracellular Thiols Sensors

Ophélie Dal Pra, Jonathan Daniel, Gaëlle Recher, Mireille Blanchard-Desce,  
Chloé Grazon

► **To cite this version:**

Ophélie Dal Pra, Jonathan Daniel, Gaëlle Recher, Mireille Blanchard-Desce, Chloé Grazon. Two-photon Dye-Based Fluorogenic Organic Nanoparticles as Intracellular Thiols Sensors. *Small Methods*, 2024, 10.1002/smt.202400716 . hal-04642514

**HAL Id: hal-04642514**

**<https://hal.science/hal-04642514v1>**

Submitted on 14 Nov 2024

**HAL** is a multi-disciplinary open access archive for the deposit and dissemination of scientific research documents, whether they are published or not. The documents may come from teaching and research institutions in France or abroad, or from public or private research centers.

L'archive ouverte pluridisciplinaire **HAL**, est destinée au dépôt et à la diffusion de documents scientifiques de niveau recherche, publiés ou non, émanant des établissements d'enseignement et de recherche français ou étrangers, des laboratoires publics ou privés.



Distributed under a Creative Commons Attribution - NonCommercial - NoDerivatives 4.0 International License

# Two-photon Dye-Based Fluorogenic Organic Nanoparticles as Intracellular Thiols Sensors

Ophélie Dal Pra, Jonathan Daniel, Gaëlle Recher, Mireille Blanchard-Desce, and Chloé Grazon\*

Optical bioimaging is an ever-growing field that benefits both from the fast progress of optical instrumentation and modalities, and from the development of light-emitting probes. The efficacy of molecular fluorescent dyes is crucial, yet hindered by limited brightness and hydrophilicity. Addressing these challenges, self-stabilized fluorogenic organic nanoparticles only made of pure dyes (*dFONs*) are introduced in this work. Comprising thiol-sensitive fluorogenic chromophores, these *dFONs* exhibit enhanced brightness exclusively in the presence of biological thiols, notably glutathione, overcoming the need for water-solubilizing moieties. Importantly, these nanoparticles demonstrate large fluorescence and one- and two-photon brightness, enabling sensitive bioimaging of intracellular thiols at micromolar concentrations. Notably, only the pristine fluorogenic nanoparticles can penetrate the cells and does not require to wash the cells before imaging, emphasizing their unique role as dye carriers, fluorogenic probes and ease of use. This work highlights the transformative potential of *dFONs* in advancing optical bioimaging, paving the way for the use of *dFONs* not just as tracers, but also now as biosensors and ultimately in the future as biomarkers.

transduction processes. Its involvement in cancers and neurodegenerative diseases also makes it an interesting target for thiol sensing systems.<sup>[1]</sup>

Among the different methods to detect thiols, fluorescence is one of the most convenient as it is versatile, cost-efficient, highly sensitive and compatible with *in vivo* biological imaging. For these reasons, several fluorescent molecular dyes were developed as fluorogenic thiol sensors:<sup>[2,3]</sup> their fluorescence is usually triggered by a chemical reaction between the dye and the nucleophilic thiols. Examples of such reactions are cyclization with aldehydes,<sup>[4]</sup> cleavage of disulfide bonds,<sup>[5]</sup> aromatic substitution-rearrangement reaction<sup>[6]</sup> or Michael additions.<sup>[7]</sup> In the latter case, using a maleimide group as the Michael acceptor, is particularly interesting as it reacts extremely rapidly ( $k = 500\text{M}^{-1}\text{s}^{-1}$ ,  $\text{pH} = 7.4$ )<sup>[8]</sup> with thiols at physiological conditions. In addition, maleimide is

an electron-acceptor group, which can potentially quench the fluorescence of electron-donating fluorescent dyes through Photo-induced electron Transfer (PeT).<sup>[9]</sup> The fluorescence is thus restored upon nucleophilic addition as the Michael adduct is no longer a good electron-acceptor. Based on this principle, several molecular thiol probes with nM to sub- $\mu\text{M}$  range Limit of Detection (LOD) were developed in fluorescence bioimaging, using structures such as coumarin ( $\text{LOD}_{\text{GSH}} = 0.5\text{ nM}$  in tris-HCl buffer,  $\text{pH} = 7.4$ ;<sup>[10]</sup>  $\text{LOD}_{\text{GSH}} = 76\text{ nM}$ ,  $\text{LOD}_{\text{Cys}} = 14\text{ nM}$ ,  $\text{LOD}_{\text{Hcy}} = 85\text{ nM}$  in PBS,  $\text{pH} = 7.4$ ),<sup>[11]</sup> triphenylamine ( $\text{LOD}_{\text{GSH}} = 85\text{ nM}$ ,  $\text{LOD}_{\text{Cys}} = 120\text{ nM}$ ,  $\text{LOD}_{\text{Hcy}} = 130\text{ nM}$  in HEPES,  $\text{pH} = 7.4$ ),<sup>[12]</sup> naphthalimide derivatives ( $\text{LOD}_{\text{GSH}} = 15\text{ nM}$ ,  $\text{LOD}_{\text{Cys}} = 12\text{ nM}$  in PBS,  $\text{pH} = 7.4$ ).<sup>[13]</sup> However, the hydrophobic backbone of these dyes limits their solubility in water and therefore requires the use of organic co-solvents (typically in between 1 and 10% of DMSO) for dissolution. The need for an organic co-solvent is a critical limitation for bioimaging purposes as it can be deleterious to the cell membrane integrity, leading to an increase cell death. In addition, the maximum brightness ( $B$ ) of such molecular dyes after thiol addition is limited to about  $10^4\text{ M}^{-1}\text{ cm}^{-1}$ . Photobleaching is another potential drawback, which may lead to poor image contrast.

One way to overcome these disadvantages is to use water-dispersible fluorescent nanoparticles. Indeed, luminescent

## 1. Introduction

Biological molecular thiols (Glutathione – GSH, Cysteine – Cys and Homocysteine -Hcy) play an important role in cellular physiology. Among them, GSH is the most abundant one with concentrations varying from the  $\mu\text{M}$  up to the  $\text{mM}$  range.<sup>[1]</sup> This antioxidant thiol plays a key role in metabolism and intracellular

O. Dal Pra, J. Daniel, M. Blanchard-Desce, C. Grazon  
Univ. Bordeaux  
CNRS  
Bordeaux INP, ISM, UMR 5255, Talence F-33400, France  
E-mail: [chloe.grazon@u-bordeaux.fr](mailto:chloe.grazon@u-bordeaux.fr)

G. Recher  
CNRS  
Univ. Bordeaux  
IOGS, LP2N, UMR 5298, Talence F-33400, France

 The ORCID identification number(s) for the author(s) of this article can be found under <https://doi.org/10.1002/smtd.202400716>

© 2024 The Author(s). Small Methods published by Wiley-VCH GmbH. This is an open access article under the terms of the [Creative Commons Attribution-NonCommercial-NoDerivs](#) License, which permits use and distribution in any medium, provided the original work is properly cited, the use is non-commercial and no modifications or adaptations are made.

DOI: 10.1002/smtd.202400716

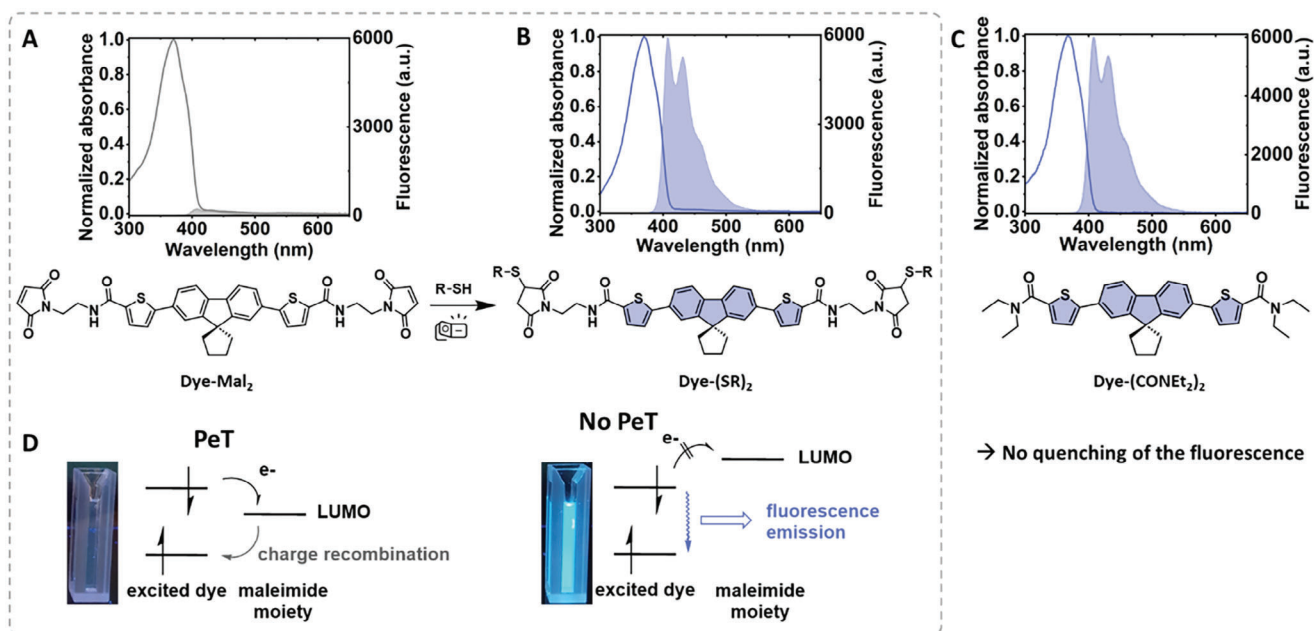


**Figure 1.** A) Absorption and fluorescence emission spectra ( $\lambda^{\text{exc}} = 365$  nm) of Bis-maleimide **Dye-Mal<sub>2</sub>** in THF. B) Absorption and fluorescence emission spectra ( $\lambda^{\text{exc}} = 365$  nm) of **Dye-(SR)<sub>2</sub>** corresponding to **Dye-Mal<sub>2</sub>** after conjugation with 2 eq. of mercaptoethanol in THF. C) Absorption and fluorescence emission spectra ( $\lambda^{\text{exc}} = 365$  nm) of Bis-diethylamide **Dye-(CONEt<sub>2</sub>)<sub>2</sub>** in THF. D) Schematic illustration of PeT from the excited dye to the maleimide moiety, inhibited after reaction with thiol (RSH).

nanoparticles are a unique class of optical nanomaterials combining large brightness and improved photostability as compared to traditional dyes. They can be intrinsically fluorescent, such as the Quantum Dots (QDs) ( $B \sim 10^2 - 10^6 \text{ M}^{-1} \text{ cm}^{-1}$ ) or made of matrices (silica, polymer) doped with dyes ( $B \sim 10^7 - 10^8 \text{ M}^{-1} \text{ cm}^{-1}$ ).<sup>[14]</sup> In the latter examples, the brightness of the particles is given by the number of dyes per particle ( $N$ ), multiplied by its molar coefficient absorption ( $\epsilon^{\text{max}}$ ) and quantum yield ( $\Phi_F$ ).<sup>[15]</sup> As a result, increasing the number of molecular emitters within a matrix will increase its brightness, as long as the fluorescent efficiency does not drop dramatically.<sup>[16,17]</sup> Only a few strategies have been developed so far to sense intracellular thiols with nanoparticles (e.g., metal organic frameworks,<sup>[18]</sup> pluronic polymers,<sup>[19]</sup> surfactants or amphiphilic polymer assemblies,<sup>[20–23]</sup> SiO<sub>2</sub><sup>[24]</sup> or MnO<sub>x</sub>-based nanomaterials,<sup>[25]</sup> nanogels,<sup>[26]</sup> gold clusters).<sup>[27,28]</sup> Most of them use UV excitation, which is detrimental to cells viability and does not allow deep light penetration. Moreover, important optical data (values of fluorescence quantum yield, absorption coefficient or brightness...) are often missing making their efficacy as in vivo sensors difficult to assess. In addition, some of these sensors are not evenly distributed in the cell cytoplasm, suggesting that some nanosensors remain into endocytic vesicles. Finally, the synthesis and formulation of these nanoprobes often requires several steps and is relatively time-consuming.

This is the reason why we set the challenge to develop thiol-sensitive fluorescent nanoparticles whose (i) preparation is accessible to each and all chemists; (ii) brightness and size are comparable to those of quantum dots; (iii) limit of detection for biological thiols is in the micromolar range, (iv) allow the use of NIR excitation for improved light penetration.

In order to meet this challenge, we turned our attention to a specific category of nanoparticles which is currently overlooked, i.e., the dye-based Fluorescent Organic Nanoparticles (*dFONs*). *dFONs* are made only of molecular dyes<sup>[29–32]</sup> and can be prepared using a simple green protocol, i.e., nanoprecipitation of dedicated hydrophobic dyes in water.<sup>[33,34]</sup> They have a number advantages over other luminescent nanoparticles including the absence of toxic components such as heavy metals (QDs), lanthanides up-conversion nanoparticles or surfactants, as well as their ease of preparation. Among *dFONs*, those made from specific dyes, i.e., (multi)polar and polarizable dyes (PPDs) are of particular interest, as they present good structural stability – due to strong dipolar interactions thanks to ultimate molecular confinement – and show high nonlinear optical responses, especially large two-photon absorption<sup>[31,35–38]</sup> which is of interest for imaging in the biological spectral window.<sup>[39]</sup> Interestingly, both their optical and their (bio)physico-chemical properties – including their chemical, photo and colloidal stabilities and their interactions with cells – critically depend on the molecular structure of the PPDs building blocks that constitute the *dFONs*.<sup>[31,35,36]</sup> Subtle engineering of their molecular structures allows reducing confinement-promoted quenching issues (also called aggregation-caused quenching),<sup>[40]</sup> while ensuring a high dye concentration condensed in a small volume. Typically, a *dFON* as small as 15 nm contains  $\approx 1500$  molecular dyes,<sup>[41]</sup> composing a tremendous pool of absorbers and fluorescent emitters. This intense absorbance and resulting brightness enables *dFONs* to rival with the brightest nanoparticles.<sup>[14,15,31]</sup> Yet, despite the growing interest in *dFONs* for various biological applications such as bioimaging (multicolor single particle tracking,<sup>[41,42]</sup> in vitro<sup>[36]</sup> or in vivo<sup>[35]</sup> two-photon imaging) or therapy

(drug-delivery,<sup>[38]</sup> photodynamic therapy,<sup>[32]</sup> photoacoustics),<sup>[43]</sup> their use as sensors are scarce and are restricted to metal cations, hydrogen peroxide or protons sensors in aqueous media.<sup>[32,44]</sup> To fill this gap, this original work presents the development of a new dye that assembles into dFONs whose fluorescence is highly sensitive to the presence of biological thiols both upon 1- and 2-photon excitation (in the NIR region) allowing detection of glutathione up to 35  $\mu\text{M}$ .

## 2. Results and Discussion

### 2.1. A Fluorogenic Dye

In the continuity of the previous work by our team,<sup>[42,45]</sup> we designed a new quadrupolar dye built from a fluorene core bearing thienyl moieties conjugated with electron-withdrawing amide end-groups. The fluorene core bears a cyclopentyl substituent in the 9 position, lying perpendicular to the extended  $\pi$ -conjugated system. As previously described, this bulky group prevents oxidation of the methylene bridge and hinders the  $\pi$ - $\pi$  stacking that would lead to aggregation-caused fluorescence quenching in confined states (i.e., solid or nanoparticle).<sup>[42,45]</sup> The dye is synthesized via a Pd-catalyzed Suzuki-Miyaura cross-coupling<sup>[42,45]</sup> between the home-made 2'-7'-diiodospiro[cyclopentane-1,9'-fluorene] and the commercially available 5-carboxythiophene-2-boronic acid pinacol ester to introduce a conjugated carboxylic acid function (Scheme S1, Supporting Information). The di-acid is then engaged in an amidation reaction in the presence of 1-(2-aminoethyl)maleimide to yield the desired bis-maleimide dye called **Dye-Mal<sub>2</sub>** (Figure 1; Figures S1–S3, Supporting Information). For comparison purpose a similar non-reactive dye named **Dye-(CONEt<sub>2</sub>)<sub>2</sub>** was also prepared (Figure 1, Scheme S2, Figures S4–S6, Supporting Information). Its photophysical characteristics are very similar to those of **Dye-Mal<sub>2</sub>** and **Dye-(SR)<sub>2</sub>**, so it can be considered a reference model (Figure 1 and Table 1). The solvatochromism of **Dye-(CONEt<sub>2</sub>)<sub>2</sub>** has also been studied (Figure S7, Supporting Information) and is assumed to be the same for **Dye-Mal<sub>2</sub>**. Dye

**Dye-Mal<sub>2</sub>** strongly absorbs in the near UV (Table 1), with a maximum peaking at 370 nm, but does not fluoresce in solution

(Figure 1). We ascribe this lack of fluorescence to a photo-induced electron transfer (PeT), as reported earlier for various dyes bearing maleimide dangling groups.<sup>[9,11,46,47]</sup> As a consequence, such dyes can be used as fluorogenic thiol probes. The maleimide moiety acts as an electron acceptor capturing an electron from the excited dye (Figure S8, Supporting Information). This is followed by a fast charge recombination resulting in fluorescence quenching. The fluorescence is recovered after the Michael addition of a thiol reagent on the maleimide unit: the maleimide dangling moieties are converted into succinimide moieties turning off the PeT process (Figure 1D). We studied the fluorescence behavior of **Dye-Mal<sub>2</sub>** in solution. Upon addition of aliquots of mercaptoethanol, we observed an increase of the fluorescence (Figure S9, Supporting Information), until it reaches a plateau after addition of 2 eq. of thiol. Such behavior has been previously observed for bis-maleimide dyes.<sup>[48]</sup> The final adduct dFONs emits in the visible blue, with a maximum peaking at 407 nm and a fluorescence quantum yield of 63% in THF, revealing a 32-fold increase compared to **Dye-Mal<sub>2</sub>**. We note that the analogous dye with diethylamide electron-withdrawing end-groups **Dye-(CONEt<sub>2</sub>)<sub>2</sub>** shows a similar photophysical behavior as **Dye-(SR)<sub>2</sub>** (Table 1), notably with a maximum emission peak at 368 nm and a fluorescence quantum yield of 62% in THF, confirming that the maleimide moieties are responsible for the quenching of fluorescence of **Dye-Mal<sub>2</sub>**.

### 2.2. A Two-Photon Absorber

One way of improving light penetration into biological tissue is to use a two-photon excitation source instead of a single-photon source as it allows to replace standard excitation in the near UV visible region by excitation at lower energy (typically in the biological spectral windows).<sup>[49]</sup> **Dye-Mal<sub>2</sub>** has also been designed to be a good two-photon absorber thanks to its quadrupolar structure provided by its fluorene electron-releasing core and its two electron-withdrawing acceptor end-groups. Based on this concept, we investigated the two-photon absorption (2PA) properties of the dye in its fluorescent form (i.e., **Dye-(SR)<sub>2</sub>**) in an organic solvent (THF). As anticipated from its

**Table 1.** Photophysical properties of **Dye-Mal<sub>2</sub>** and **Dye-(SR)<sub>2</sub>** in THF and of dFONs-Mal before and after reactions with biologically relevant thiols (i.e., dFONs-GSH, dFONs-Cys and dFONs-Hcy) in water.

Sample	$\lambda_{abs}^{max}$ nm	$\epsilon^{max}$ <sup>a)</sup> $10^3 \text{ M}^{-1} \text{ cm}^{-1}$	FWHM <sup>b)</sup> $\text{cm}^{-1}$	Stokes' shift $\text{cm}^{-1}$	$\lambda_{em}^{max}$ nm	$\Phi_F$ <sup>c)</sup> %	$\epsilon^{max} \Phi_F$ <sup>d)</sup> $10^3 \text{ M}^{-1} \text{ cm}^{-1}$	$\lambda_{2PA}^{max}$ nm	$\sigma_{2PA}^{max}$ <sup>e)</sup> GM	$\sigma_{2PA}^{max} \Phi_F$ <sup>f)</sup> GM
Dye-Mal <sub>2</sub>	370	59 ± 5	4160	2460	407	<2	<1.2	/	/	/
Dye-(SR) <sub>2</sub>	370	59 ± 5	4160	2460	407	63 ± 4	37	<680	>123 ± 8	>77
Dye-(CONEt <sub>2</sub> ) <sub>2</sub>	368	60 ± 5	4120	2660	408	62 ± 5	37	/	/	/
dFONs-Mal	360	40 ± 5	7300	6040	460	<1	<0.4	/	/	/
dFONs-CONEt <sub>2</sub>	336	33 ± 5	3560	8120	462	3 ± 1	1.9	/	/	/
dFONs-GSH	372	40 ± 5	5950	4900	455	35 ± 8	14	680	13	4
dFONs-Cys	360	30 ± 5	8100	6370	467	6 ± 2	1.8	/	/	/
dFONs-Hcy	344	33 ± 5	8460	7560	465	4 ± 1	1.4	/	/	/

<sup>a)</sup> Molar absorption coefficient of the dyes (in solution in DMSO or as dFONs subunits), error bars correspond to n = 3 independent  $\epsilon$  measurements (three different dyes stock solutions); <sup>b)</sup> Full Width at Half Maximum; <sup>c)</sup> Fluorescence quantum yield, average and standard deviation for n = 3 measurements on n = 3 different batches of dFONs (pristine or reacted with thiols). Reference: Quinine bisulfate (QBS)  $\Phi_F = 0.546$  in H<sub>2</sub>SO<sub>4</sub> 0.5 M; <sup>d)</sup> Dye brightness; <sup>e)</sup> Dye two-photon absorption cross-section at 2PA maximum ( $\lambda_{2PA}^{max}$ ), value of **Dye-(SR)<sub>2</sub>** corresponds to the average of n = 2 measures and standard deviation; <sup>f)</sup> Dye two-photon brightness.

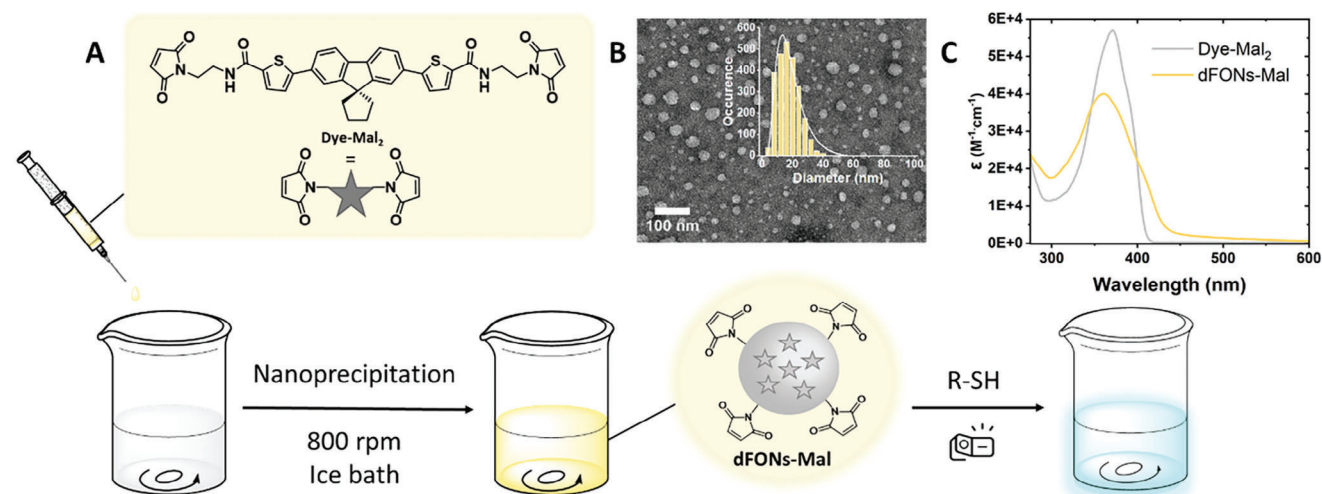


**Figure 2.** A) Schematic illustration of the nanoprecipitation process yielding dye-based fluorogenic organic nanoparticles (*dFONs-Mal*) made of **Dye-Mal<sub>2</sub>** and their fluorogenic character after reaction with a thiol. B) Typical TEM image of the corresponding *dFONs* ( $17 \pm 7$  nm) and histogram associated ( $n = 2519$  counts). C) Absorbance spectra of **Dye-Mal<sub>2</sub>** in THF (gray) and *dFONs-Mal* in water (yellow).

quadrupolar structure,<sup>[31,50,51]</sup> the centrosymmetry of the dye results in a sensible 2PA response in the NIR ( $\sigma_2^{\max} \geq 130$  GM,  $\lambda_{2PA}^{\max} < @680$  nm) associated with a blue-shift of the 2PA absorption as compared with twice the 1PA low-energy absorption band (Table 1 and Figure S10, Supporting Information).

### 2.3. Fluorogenic Organic Nanoparticles

**Dye-Mal<sub>2</sub>** was then nanoprecipitated in water to yield the corresponding *dFONs-Mal* (Figure 2). Typically, a minute amount of a stock solution of the **Dye-Mal<sub>2</sub>** in a water-miscible organic solvent (here THF) is added under magnetic stirring to a large volume of distilled water. A non-turbid colloidal suspension is instantaneously obtained. Due to the “polar and polarizable” nature of the dye, such *dFONs* should show a strong structural cohesion facilitated by intermolecular interactions, notably of a dipolar nature. These interactions are significant due to the close proximity of the confined dyes.<sup>[31]</sup> Transmission Electron Microscopy (TEM) experiments confirms the presence of a population of spherical nanoparticles with an average dry diameter of  $17 \pm 7$  nm. From this diameter we can deduce that each nanoparticle contains around 2000 dyes (Equation S1, Supporting Information), corresponding to a concentration of *dFONs-Mal* in water of 2 nM (see experimental section). *In the rest of this article, this will be referred as the nanoprobe concentration.* The absorption spectrum of *dFONs-Mal* in water is presented Figure 2C. In comparison to the absorption of **Dye-Mal<sub>2</sub>** dissolved in THF we observe a broadening (FWHM increases by 175%) and a hypsochromic shift of 10 nm (i.e.,  $750 \text{ cm}^{-1}$ ) of the low-energy absorption band of *dFONs-Mal*, as well as a hypochromic shift with a molar absorption coefficient dropping from  $59000 \text{ M}^{-1} \text{ cm}^{-1}$  for **Dye-Mal<sub>2</sub>** to  $40000 \text{ M}^{-1} \text{ cm}^{-1}$  for *dFONs-Mal* (Table 1; Figures 2C and S11, Supporting Information). These modifications are the signature of excitonic splitting phenomena that are favored by the close proximity of the dyes confined in *dFONs*.<sup>[52]</sup> Briefly, the low-energy absorption

band is broadened due to the overlap of the two bands originating from the transition to the lower excitonic split excited state and to the higher excitonic split excited state. The relative intensity of these two bands depends on the relative orientation of the dyes in close proximity (typically only the low-energy one is allowed in J-type (in line) aggregate whereas only the high-energy one is allowed in H-type (card-pack) aggregate, with both bands being allowed with varying transition dipoles depending on the relative orientation of the dyes).<sup>[52]</sup> In addition, *dFONs-Mal* barely fluoresce as a result of PeT occurring also in *dFONs*. The blue-shift is even more noticeable in the case of *dFONs* made from the unreactive **Dye-(CONEt<sub>2</sub>)<sub>2</sub>** (Figure S11, Supporting Information). As expected, we observe a significant red-shift of the emission (originating from the much less allowed low-energy excited state) along with a decrease in fluorescence quantum yield compared to the free dye in solution.

When adding a thiol on the maleimide moiety of the nanoparticles, the PeT is turned off leading to a cyan restored fluorescence (Figures 2 and 3). Based on these results, we thus proceed to explore their possible use as fluorogenic sensors of biologically relevant thiols.

### 2.4. Spectral Responses of *dFONs-Mal* toward Thiols

The reactivity of *dFONs-Mal* (2 nM) toward intracellular thiols was first evaluated in HEPES buffer using glutathione (GSH – 50  $\mu\text{M}$ ). After 6 h (pH = 7.4, 25 °C), the colloidal dispersion emits a blue fluorescence, revealing the grafting of the thiol onto the maleimide *dFONs*. As with most maleimide-based fluorogenic probes, the higher the pH, the more intense the fluorescence response to GSH (Figure S12, Supporting Information). For most of the remaining experiments of this study we chose a pH = 7.4 to mimic the cells environments. More precisely, at pH = 7.4, the *dFONs-Mal* having reacted with GSH (hereafter designated by *dFONs-GSH*) present

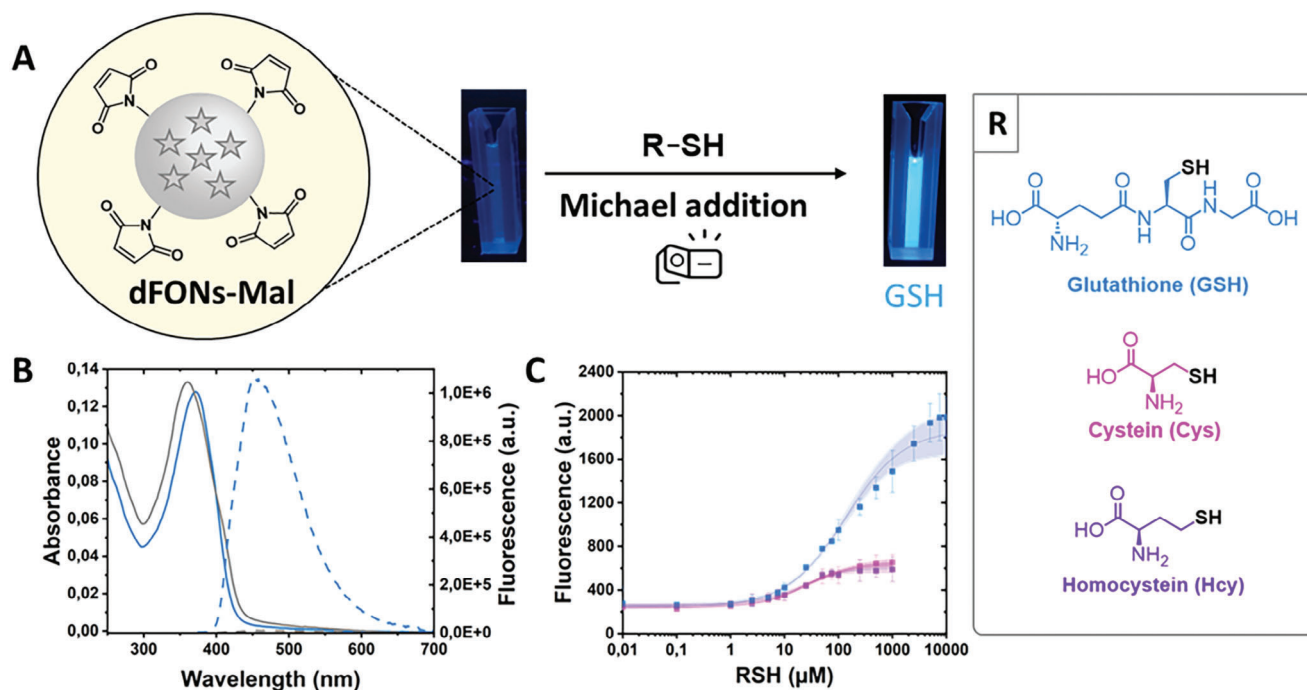


**Figure 3.** A) Schematic illustration of the fluorescence enhancement after reaction of *dFONs-Mal* with GSH in HEPES buffer (pH = 7.4). B) Absorbance (solid line) and emission (dashed line) of *dFONs-Mal* (grey) and *dFONs-GSH* (blue), i.e., *dFONs-Mal* after reaction with GSH. C) Fluorescence dose-response curve of *dFONs-Mal* reacted with three different biological thiols (GSH, Cys and Hcy) in cell culture media (DMEM) at 37 °C for 20 min. The points and errors bars correspond to the average and standard deviation values of  $n = 3$  different batches of *dFONs* reacted with thiols.

a similar absorption spectrum as pristine *dFONs-Mal* ( $\lambda_{\text{abs}}^{\text{max}} = 372 \text{ nm}$ ) but are strongly emitting in the blue region (Figure 3). *dFONs-GSH* indeed show an intense blue fluorescence ( $\lambda_{\text{em}}^{\text{max}} = 455 \text{ nm}$ ) with a fluorescence quantum yield of 35%, reflecting a fluorescence enhancement by a factor over 30 compared to *dFONs-Mal*. Interestingly, using the same reaction conditions, the *dFONs-Mal* having reacted with Cys or Hcy (Figure S13, Supporting Information) only exhibits a 4 to 5 folds fluorescence enhancement.

To the best of our knowledge, this is the first time that a single component fluorogenic nanoparticle sensing biologically relevant thiols is reported.

Disadvantages of maleimides are their sensitivity towards hydrolysis (i) and their possible nucleophilic attack by amines (ii), which might be a potential limitation for probe storage and intracellular detection since the cell medium contains amino-acids (Table S1, Supporting Information). To assess this *drawbacks*, (i) we first explored the *dFONs*' optical, colloidal and chemical stability by recording its absorbance and fluorescence emission in different aqueous media over time (Figure S14, Supporting Information): a decrease in the absorbance value would indicate sedimentation or chemical degradation of the *dFONs* and the apparition of a scattering background would indicate aggregation of the nanoparticles; in the case of this maleimide probe, an increase of the fluorescence would indicate an hydrolysis by the hydroxide ions. Our results demonstrate that *dFONs-Mal* are colloiddally stable over 24 h in storage media as ultra-pure water or HEPES 25 mM at room temperature and show no to very little hydrolysis in those conditions (Figure S14A,B,E, Supporting Information). In addition, *dFONs-Mal* stored in ultra-pure wa-

ter are colloiddally stable up to 6 months at 4 °C in the dark and show limited hydrolysis over time (~15% of the fluorescence is restored compared to a reaction with GSH, Figure S14F, Supporting Information). Such results indicate that we can use the probe several weeks after its preparation. In cell-compatible media as PBS 1x or DMEM, *dFONs-Mal* are chemically stable, although in DMEM an increase in fluorescence is observed from the very start (Figure S14D, Supporting Information) also shown in the Figure S15 (Supporting Information) (control conditions). In addition, *dFONs-Mal* are perfectly colloiddally stable in PBS (Figure S14C, Supporting Information) but less so in DMEM (decrease in absorbance, see Figure S14D, Supporting Information), showing that *dFONs-Mal* must be rapidly used after being brought into contact with the medium, which is not an issue as *dFONs* are internalized by the cells in less than 30 min (*vide infra*).

Second, (ii) we investigated the reaction of *dFONs-Mal* with thiols in a cell culture medium and determined the thiol detection threshold of our nanoprobe in such an environment. *dFONs-Mal* were first reacted with GSH, Cys and Hcy in DMEM at 37 °C and the fluorescence was recorded over time. In all cases, the fluorescence increases and reaches a plateau after 15 min (Figure S15, Supporting Information). Interestingly, in the cell culture medium, *dFONs-GSH* are still around twice brighter than *dFONs-Cys* and *dFONs-Hcy*. They also are three times brighter than the *dFONs-Mal* left to evolve in the cell culture medium for the same duration.

Next, we investigated the nanoprobe limit of detection for GSH, Cys and Hcy by studying the fluorescence intensity of *dFONs-Mal* after 20 min at 37 °C in DMEM as a function of

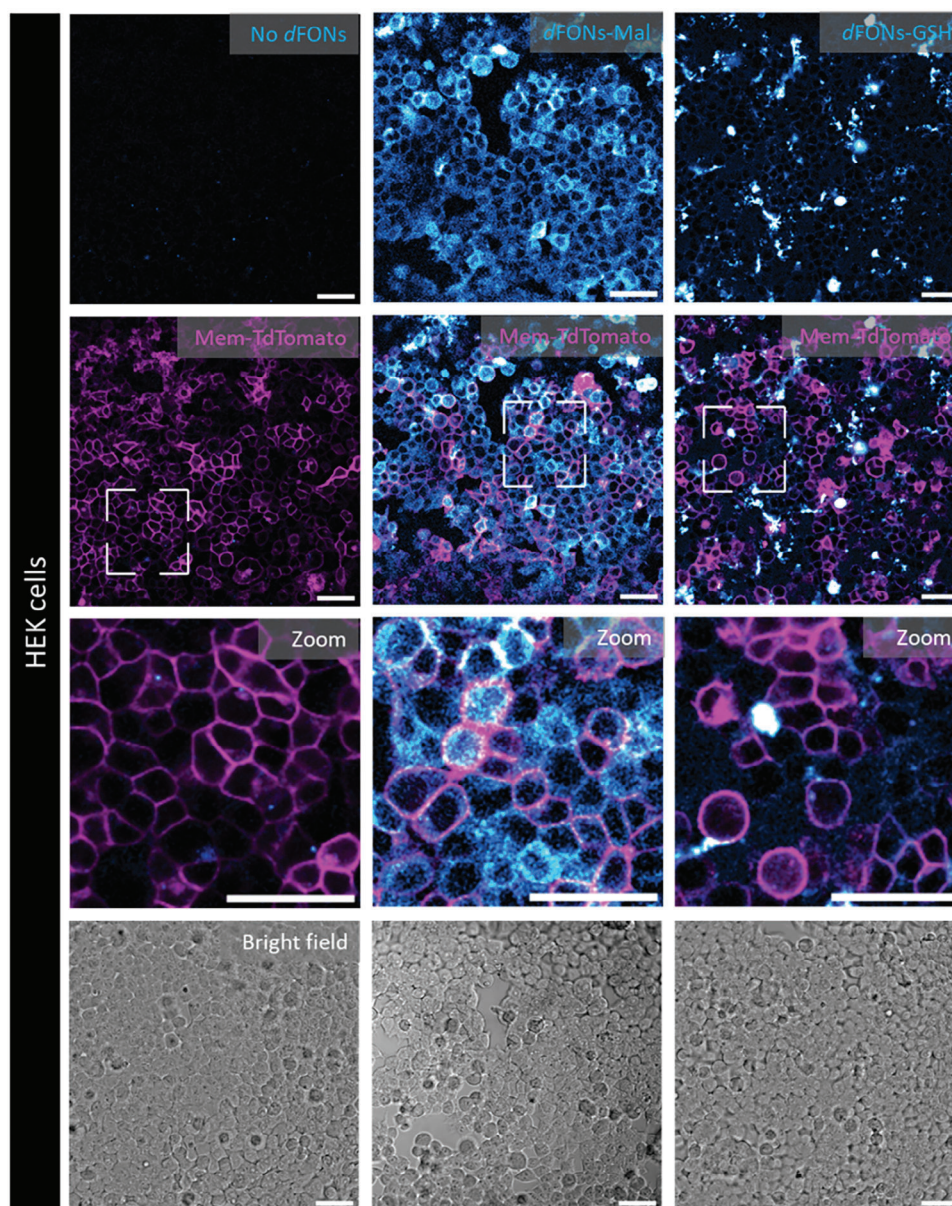


**Figure 4.** HEK cells incubated 30 min with *dFONs-Mal* (2 nM) or *dFONs-GSH* (2 nM) in DMEM culture medium, at 37 °C,  $\lambda^{\text{exc}} = 405$  nm (cyan channel corresponding to *dFONs-Mal* emission and magenta channel to TdTomato labelled membrane). Scale bar 50  $\mu\text{m}$ .

initially added thiols concentrations (Figure 3C). The detection limit for GSH in biological conditions is found to be 35  $\mu\text{M}$  (Equations S2, S3, S4, Figure S16, Supporting Information).<sup>[53]</sup> The dose-response curves also confirm that *dFONs-Mal* are more sensitive to GSH than to Cys or Hcy. Therefore, given the higher reactivity of our nanoprobe towards GSH and the high intracellular concentration of GSH (1–10 mM) compared to Cys (30–200  $\mu\text{M}$ ) and Hcy (5–12  $\mu\text{M}$ ), we can state that our probe will almost exclusively sense intracellular GSH. Our probe is not the most performant in terms of detection limit, as other molecular probes based on maleimides have LODs in the order of nM (see introduction paragraph for details). However, it is difficult to make rigorous comparison among sensors since the LODs have not been measured under the same conditions of

exposition time, temperature, pH, nature of the medium (often ultra-pure water, whereas our medium is directly cell culture). Moreover, the value of the LOD also depends on the spectrophotometer performances (signal/noise ratio).<sup>[54]</sup> The interest of our sensor lies in its extreme brightness compared to the literature and the absence of organic cosolvent required for its use (vide infra), a real advantage for tests in biological environments.

The ex-vitro experiments confirmed that the nanoprobe *dFONs-Mal* is highly reactive towards biologically relevant thiols at 37 °C, outperforming existing competitors (amino-acids, vitamins, water). In addition, the nanoprobe range of detection for GSH is extremely large (10  $\mu\text{M}$  to 10 mM, Figure 3C), which is very promising for its use as an intracellular biosensor.

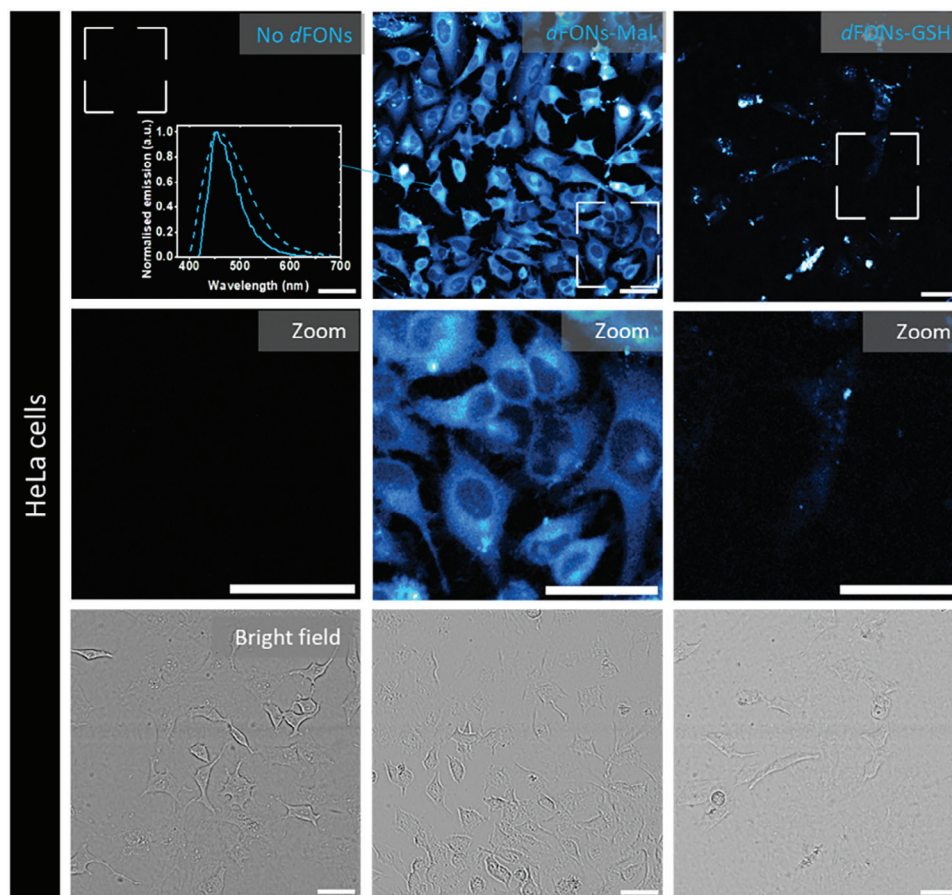


**Figure 5.** HeLa cells incubated 30 min with *dFONs-Mal* (2 nM) or *dFONs-GSH* (2 nM) in DMEM culture medium, at 37 °C,  $\lambda^{\text{exc}} = 405$  nm (cyan channel corresponding to *dFONs-Mal* emission). Scale bar 50  $\mu\text{m}$ . Insert: Normalized emission spectra of *dFONs-Mal* inside the HeLa cells (solid line- $\lambda$ -scan) superimposed with *dFONs-GSH* fluorescence emission in HEPES buffer (dashed line, see Figure S18 (Supporting Information) for higher resolution graph).

### 2.5. Sensing Intra-Cellular Biological Thiols

In order to assess the cell permeability and capability of the nanoprobe *dFONs-Mal* to selectively detect intracellular thiols, live cells imaging studies were performed using two different human cells lines: HEK293T embryonic kidney-derived cells (Figure 4) and HeLa cancer cells (Figure 5). First, we ensured that our probe (2 nM) was cytocompatible with the different cell lines over the experimental time ( $\approx 2$  h, see Figure S17, Supporting Information). The cells were then incubated with the *dFONs-Mal* (2 nM) for 30 min in DMEM medium at 37 °C and then directly imaged without any washing step. Upon excitation at 405 nm, a significant homogeneous signal of fluorescence appears inside both type of cells proving the rapid internalization of *dFONs-Mal* inside HEK and HeLa cells after only 30 min incubation. The fluorescence signal is most probably due to the reaction of the probe with the intracellular thiols. As a control experiment, the cells alone were imaged and almost no fluorescence emission was observed in the same conditions, indicating that the signal is due to the reacting probe and not to cell autofluorescence. In addition, the emission spectrum of the nanoparticles was recorded inside the HeLa cells (insert Figure 5, Figure S18, Supporting Information) and it superimposed well on the spectrum of the *dFONs-*

*GSH* grafted in HEPES buffer at 37 °C, confirming once again that the emission observed is indeed that of the *dFONs* that had reacted with the intracellular thiols.

Therefore, *dFONs-Mal* probes can detect thiols both in cancerous or non-cancerous cells. Furthermore, *dFONs-GSH*, i.e., *dFONs-Mal* previously reacted with GSH, were also incubated in the cells in the same conditions. Surprisingly, we could not observe any cell internalization, meaning that only the pristine *dFONs-Mal* can be internalized into cells. In contrast, *dFONs-GSH* seem to slightly non-specifically adsorb onto HEK cells membrane, while almost no fluorescence signal is measured for HeLa cells. Hence *dFONs-Mal* are not only capable of detecting intracellular thiols, but also react only with the thiols that are located inside the cells and act as nanocarriers.

### 2.6. Two-Photon Excitation and Imaging

To get rid of the excitation of the endogenous species ( $\lambda^{\text{exc}} = 405$  nm), we exploited the non-linear optical properties of our dyes and of *dFONs* made from them using near-IR two-photon excitation (2P). First, we measured the two-photon absorption (2PA) properties of the fluorescent *dFONs-GSH* in aqueous

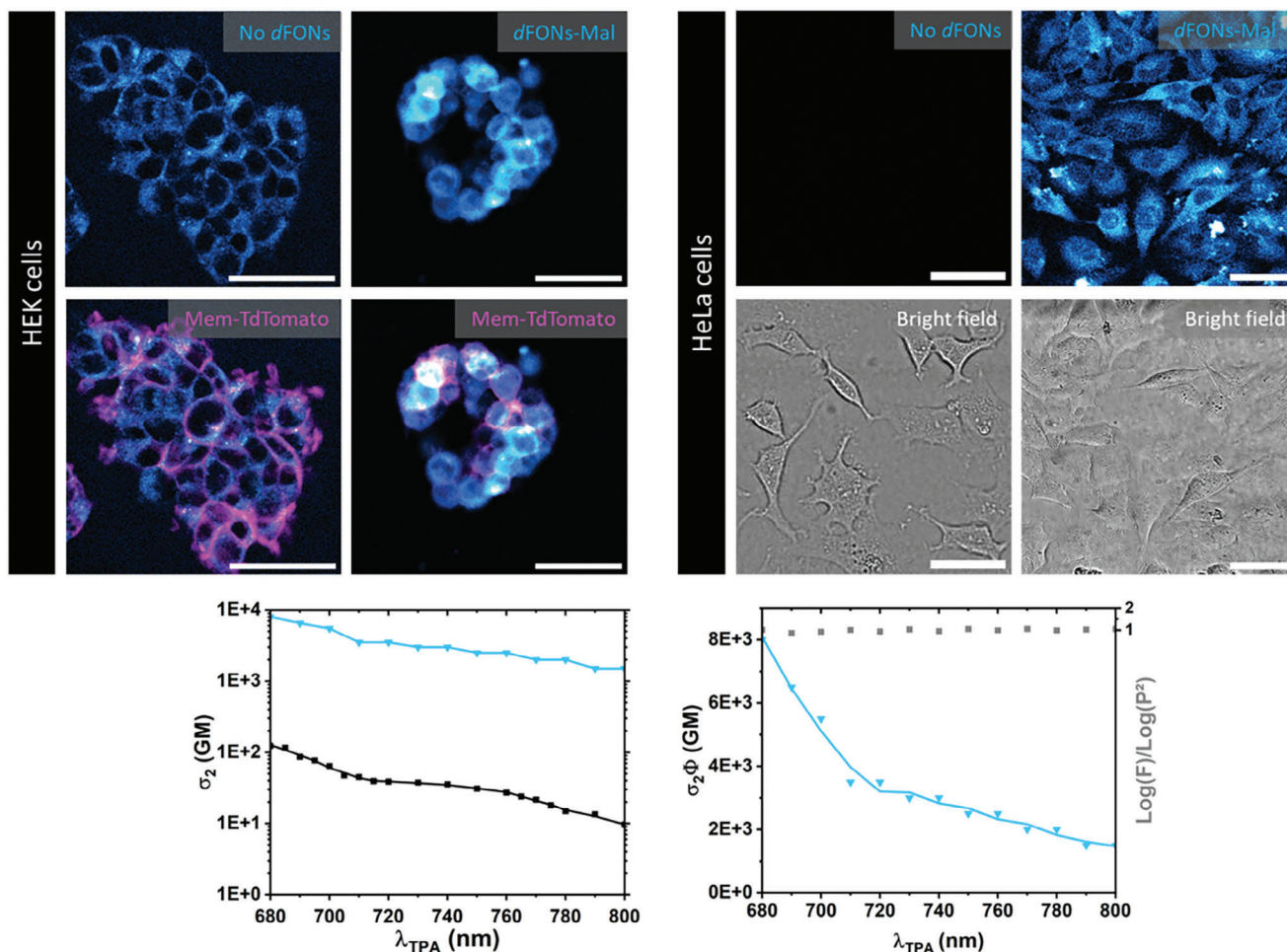


**Figure 6.** Top: two-photon excited fluorescence images of HEK cells (left, membrane labelled with TdTomato) or HeLa cells (right) after 30 min of incubation with 2 nM of *dFONs-Mal* in DMEM at 37 °C at  $\lambda_{exc,2P} = 780$  nm, and associated control experiments (no *dFONs*, cells alone). Bottom: two-photon brightness spectra of *dFONs-GSH* (blue triangles & line) in HEPES buffer. The quadratic dependency of the fluorescence signal with laser power (grey square) is expressed as  $\log(F)/\log(P^2)$ . Superposition of two-photon absorption spectra of *Dye-(SR)<sub>2</sub>* in THF (black dots) and of *dFONs-GSH* in HEPES buffer (blue triangle).

(HEPES buffer, pH = 7.4) (Figure 6). Despite the decrease in the two-photon absorption of the dyes upon molecular confinement, the overall *dFONs-GSH* brightness amounts to 8000 GM at 680 nm, thanks to the large number of dyes per nanoparticle and its large fluorescence quantum yield. We stress that this two-photon brightness value is about 40 fold higher than the one of the brightest 2P thiol probe reported so far (BODIPY derivative, Table S2, Supporting Information).<sup>[55]</sup> This probe has a LOD of 25 nM for GSH but is not soluble in water, thus requiring a large amount of co-solvent for the cells experiments. A naphthalimide-derivative with a maleimide dandling group was also reported with an emission wavelength of 470 nm and a 2P brightness of 22 GM.<sup>[56]</sup> Unlike our sensor, this dye maleimide only reacts with Cys with a LOD of 5 nM, not with GSH or Hcy. Other dye-based two-photon thiol probe have been developed but they present lower 2P brightness, or either their 2P absorbance and brightness is not reported, either their LOD, restricting a comparison of both photophysical and sensing properties with our nanoprobe (Table S2, Supporting Information). In additions, all these probes have a low

water solubility and also requires a co-solvent for aqueous studies. Finally, two thiol nanosensors have been developed. One is an organic hydrogel containing dyes,<sup>[26]</sup> while the other one is a metallic nanoparticle.<sup>[28]</sup> They both sense GSH or Cys around 2–180 nM and are perfectly water-dispersible. However, once again their quantum yield and absorbance properties are missing.

As *dFONs-Mal* nanoparticles are both good two-photon absorbers, and thiol sensors, live-cell imaging was also performed with two-photon excitation condition ( $\lambda_{exc} = 780$  nm) using a highly diluted solution of *dFONs* (2 nM). The images were obtained after incubation of *dFONs-Mal* for 30 min at 37 °C with both cells' lines (HEK and HeLa, Figure 6). Cellular imaging shows the ability of *dFONs-Mal* to (i) be quickly internalized within cells, (ii) react with the intracellular biological thiols and (iii) consequently allow thiol detection using NIR excitation thanks to its fluorogenic property and large two-photon absorption. These results demonstrate that *dFONs-Mal* are promising tools for more advanced biological applications, i.e., detection into tissues or scattering media (i.e., urine, blood, plasma).<sup>[31]</sup>

### 3. Conclusion

In conclusion, we designed an original maleimide-dye which initially does not fluoresce, due to a PeT quenching mechanism. Once nanoprecipitated in water, this dye leads to small (<30 nm), non-fluorescent, **dFONs-Mal** nanoparticles which in presence of biologically relevant thiols, become emissive. As far as we know, this fluorogenic **dFONs-Mal** is also one of the very few examples of fluorogenic dye-based nanoparticles developed to date.<sup>[57]</sup> In addition, the nanoprobe is perfectly compatible with physiological temperatures and supplemented biological media. In particular, the high sensitivity of **dFONs-Mal** regarding GSH (35  $\mu$ M) and its large dynamic range (10  $\mu$ M to 10 mM) makes it an ideal probe for intracellular thiols level measurements. Based on these results, we investigated the behavior of this nanoprobe in intracellular environment. Using only 2 nM of probe, and after 30 min incubation, **dFONs-Mal** are internalized into cells, regardless of the lineage (HeLa or HEK) and without requiring any washing step. The distribution of fluorescence is homogeneous within the cells. Furthermore, the **dFONs-Mal** having previously reacted with GSH are not internalized in the cells, but instead either are non-specifically adsorbed onto the cell membrane (HEK), or do not interact at all with cells (HeLa). These very original results suggest that our nanoprobe can only penetrate cells in its native form and is therefore only specific to intracellular thiols.

Moreover, the **dFONs-GSH** can be excited in the NIR region, and present a two-photon brightness of 8000 GM, allowing successful two-photon imaging of intracellular thiols within cells. As such they represent promising tools for sensing thiols in turbid media and to complete the arsenal of nanotools for early diagnostic and monitoring of neurodegenerative disorders.

### Supporting Information

Supporting Information is available from the Wiley Online Library or from the author.

### Acknowledgements

This work was supported by the ERC COMET (101077364), and the University of Bordeaux Matter and Radiation Sciences Department. Financial support for Ophélie Dal Pra was provided through the MENESR (Ministère de l'Éducation Nationale, de l'Enseignement Supérieur et de la Recherche) of France. The Conseil général d'Aquitaine was also acknowledged for financial support (Chaire d'Excellence Grant to MBD). M. B-D. and G. R. were supported by the CNRS MITI "Défi Auto-Organisation" grant. G. R. acknowledges the GdR ImaBio for support, and the ANR for funding (ANR-21-CE19-0029). Continuous support from Univ. Bordeaux, CNRS and Bordeaux-INP was greatly acknowledged. Adeline Boyreau (LP2N-Bordeaux) was greatly acknowledged for her cautious care of HEK cells and the preparation of the samples prior to the experiment, Laetitia Andrique for the design of the lentiviral construct used to stain HEK cells and Julie Angibaud and Morgane Rosendale (IINS, Bordeaux, France) for kindly providing HeLa cells (purchased from ATCC). The authors also thanks Aissam Okba for synthesizing the **Dye-(CONET<sub>2</sub>)<sub>2</sub>**, Frédéric Friscourt and Zoeisha Chinoy for their help on the fluorescence plate reader measurements, Amaury Badon for his help with TEM analysis with Python and Marine Lavainne and Laurent Bouffier for their help with the cyclic voltammetry measurements.

### Conflict of Interest

The authors declare no conflict of interest.

### Data Availability Statement

The data that support the findings of this study are openly available in CNRS (FR) at <https://mycore.core-cloud.net/index.php/s/gdjZ3CmrSsceiQu>, reference number [DOI 10.1002-smtd.202400716].

### Keywords

bioimaging, biosensors, cellular imaging, luminophore, wash-free probes

Received: May 15, 2024

Revised: June 26, 2024

Published online:

- [1] S. Wang, Y. Huang, X. Guan, *Molecules* **2021**, *26*, 3575.
- [2] L.-Y. Niu, Y.-Z. Chen, H.-R. Zheng, L.-Z. Wu, C.-H. Tung, Q.-Z. Yang, *Chem. Soc. Rev.* **2015**, *44*, 6143.
- [3] J. Dai, C. Ma, P. Zhang, Y. Fu, B. Shen, *Dyes Pigment.* **2020**, *177*, 108321.
- [4] O. Rusin, N. N. St. Luce, R. A. Agbaria, J. O. Escobedo, S. Jiang, I. M. Warner, F. B. Dawan, K. Lian, R. M. Strongin, *J. Am. Chem. Soc.* **2004**, *126*, 438.
- [5] L. Yang, W. Qu, X. Zhang, Y. Hang, J. Hua, *Analyst* **2015**, *140*, 182.
- [6] L.-Y. Niu, Y.-S. Guan, Y.-Z. Chen, L.-Z. Wu, C.-H. Tung, Q.-Z. Yang, *J. Am. Chem. Soc.* **2012**, *134*, 18928.
- [7] H. S. Jung, T. Pradhan, J. H. Han, K. J. Heo, J. H. Lee, C. Kang, J. S. Kim, *Biomaterials* **2012**, *33*, 8495.
- [8] J. M. J. M. Ravasco, H. Faustino, A. Trindade, P. M. P. Gois, *Chem. – A Eur. J.* **2019**, *25*, 43.
- [9] T. Matsumoto, Y. Urano, T. Shoda, H. Kojima, T. Nagano, *Org. Lett.* **2007**, *9*, 3375.
- [10] L. Yi, H. Li, L. Sun, L. Liu, C. Zhang, Z. Xi, *Angew. Chem., Int. Ed.* **2009**, *48*, 4034.
- [11] Z. Chen, Q. Sun, Y. Yao, X. Fan, W. Zhang, J. Qian, *Biosens. Bioelectron.* **2017**, *91*, 553.
- [12] T. Liu, F. Huo, C. Yin, J. Li, J. Chao, Y. Zhang, *Dyes Pigment.* **2016**, *128*, 209.
- [13] J. Qian, G. Zhang, J. Cui, L. Zhou, Z. Chen, Z. Zhang, W. Zhang, *Sens. Actuators, B* **2020**, *311*, 127923.
- [14] W. R. Algar, M. Massey, K. Rees, R. Higgins, K. D. Krause, G. H. Darwish, W. J. Peveler, Z. Xiao, H.-Y. Tsai, R. Gupta, K. Lix, M. V. Tran, H. Kim, *Chem. Rev.* **2021**, *121*, 9243.
- [15] A. H. Ashoka, I. O. Aparin, A. Reisch, A. S. Klymchenko, *Chem. Soc. Rev.* **2023**.
- [16] C. Grazon, J. Rieger, R. Méallet-Renault, B. Charleux, G. Clavier, *Macromolecules* **2013**, *46*, 5167.
- [17] C. Grazon, J. Rieger, B. Charleux, G. Clavier, R. Méallet-Renault, *J. Phys. Chem. C* **2014**, *118*, 13945.
- [18] Y.-A. Li, C.-W. Zhao, N.-X. Zhu, Q.-K. Liu, G.-J. Chen, J.-B. Liu, X.-D. Zhao, J.-P. Ma, S. Zhang, Y.-B. Dong, *Chem. Commun.* **2015**, *51*, 17672.
- [19] L. Wang, S. Zhuo, H. Tang, D. Cao, *Sens. Actuators, B* **2018**, *277*, 437.
- [20] M. Ye, X. Wang, J. Tang, Z. Guo, Y. Shen, H. Tian, W.-H. Zhu, *Chem. Sci.* **2016**, *7*, 4958.
- [21] H. Wang, P. Zhang, C. Zhang, S. Chen, R. Zeng, J. Cui, J. Chen, *Mater. Adv.* **2020**, *1*, 1739.
- [22] C. Y. Ang, S. Y. Tan, Y. Lu, L. Bai, M. Li, P. Li, Q. Zhang, S. T. Selvan, Y. Zhao, *Sci. Rep.* **2014**, *4*, 7057.

- [23] Z. Ning, S. Wu, G. Liu, Y. Ji, L. Jia, X. Niu, R. Ma, Y. Zhang, G. Xing, *Chem. – An Asian J.* **2019**, *14*, 2220.
- [24] H.-J. Wu, C.-C. Chang, *Molecules* **2020**, *25*, 5732.
- [25] Y.-W. Bao, X.-W. Hua, J. Zeng, F.-G. Wu, *Research* **2020**, 2020, <https://spj.science.org/doi/10.34133/2020/9301215>.
- [26] X. Guo, X. Zhang, S. Wang, S. Li, R. Hu, Y. Li, G. Yang, *Anal. Chim. Acta* **2015**, *869*, 81.
- [27] X. Zhang, F.-G. Wu, P. Liu, N. Gu, Z. Chen, *Small* **2014**, *10*, 5170.
- [28] P. Zhang, J. Wang, H. Huang, H. Chen, R. Guan, Y. Chen, L. Ji, H. Chao, *Biomaterials* **2014**, *35*, 9003.
- [29] A. Patra, C. G. Chandaluri, T. P. Radhakrishnan, *Nanoscale* **2012**, *4*, 343.
- [30] S. Fery-Forgues, *Nanoscale* **2013**, *5*, 8428.
- [31] J. Daniel, O. Dal Pra, E. Kurek, C. Grazon, M. Blanchard-Desce, *Comptes. Rendus de Chimie* **2024**, *27*, 1.
- [32] A. Chaudhuri, A. Paul, A. Sikder, N. D. P. Singh, *Chem. Commun.* **2021**, *57*, 1715.
- [33] H. Masuhara, H. Nakanishi, K. Sasaki, *Single Organic Nanoparticles*; Springer-Verlag Berlin Heidelberg, 2003. pp. XLIX, 402.
- [34] D. Horn, J. Rieger, *Angew. Chem., Int. Ed.* **2001**, *40*, 4330.
- [35] V. Parthasarathy, S. Fery-Forgues, E. Campioli, G. Recher, F. Terenziani, M. Blanchard-Desce, *Small* **2011**, *7*, 3219.
- [36] P. Pagano, M. Rosendale, J. Daniel, J.-B. Verlhac, M. Blanchard-Desce, *J. Phys. Chem. C* **2021**, *125*, 25695.
- [37] M. Rosendale, J. Daniel, F. Castet, P. Pagano, J.-B. Verlhac, M. Blanchard-Desce, *Molecules* **2022**, *27*, 2230.
- [38] J. Boucard, C. Linot, T. Blondy, S. Nedellec, P. Hulin, C. Blanquart, L. Lartigue, E. Ishow, *Small* **2018**, *14*, 1802307.
- [39] A. M. Smith, M. C. Mancini, S. Nie, *Nat. Nanotech.* **2009**, *4*, 710.
- [40] J. Gierschner, J. Shi, B. Milián-Medina, D. Roca-Sanjuán, S. Varghese, S. Park, *Adv. Opt. Mater.* **2021**, *9*, 2002251.
- [41] M. Rosendale, J. Flores, C. Paviolo, P. Pagano, J. Daniel, J. Ferreira, J. Verlhac, L. Groc, L. Cognet, M. Blanchard-Desce, *Adv. Mater.* **2021**, *33*, 2006644.
- [42] J. Daniel, A. G. Godin, M. Palayret, B. Lounis, L. Cognet, M. Blanchard-Desce, *J. Phys. D: Appl. Phys.* **2016**, *49*, 084002.
- [43] Y. Cai, P. Liang, Q. Tang, X. Yang, W. Si, W. Huang, Q. Zhang, X. Dong, *ACS Nano* **2017**, *11*, 1054.
- [44] M. Ahmed, M. Faisal, A. Ihsan, M. M. Naseer, *Analyst* **2019**, *144*, 2480.
- [45] H. Li, J. Daniel, J.-B. Verlhac, M. Blanchard-Desce, N. Sojic, *Chem. – A Eur. J.* **2016**, *22*, 12702.
- [46] X. Wu, H. Shu, B. Zhou, Y. Geng, X. Bao, J. Zhu, *Sens. Actuators, B* **2016**, *237*, 431.
- [47] Z. Wang, Z. Huang, N. Zhou, X.-H. Dong, X. Zhu, Z. Zhang, *Polym. Chem.* **2017**, *8*, 2346.
- [48] S. Girouard, M.-H. Houle, A. Grandbois, J. W. Keillor, S. W. Michnick, *J. Am. Chem. Soc.* **2005**, *127*, 559.
- [49] F. Helmchen, W. Denk, *Nat. Methods* **2005**, *2*, 932.
- [50] M. Albota, D. Beljonne, J. L. Brédas, J. E. Ehrlich, J. Y. Fu, A. A. Heikal, S. E. Hess, T. Kogej, M. D. Levin, S. R. Marder, D. McCord-Maughon, J. W. Perry, H. Röckel, M. Rumi, G. Subramaniam, W. W. Webb, X. L. Wu, C. Xu, *Science* **1998**, *281*, 1653.
- [51] F. Terenziani, C. Katan, E. Badaeva, S. Tretiak, M. Blanchard-Desce, *Adv. Mater.* **2008**, *20*, 4641.
- [52] M. Kasha, H. R. Rawls, M. A. El-Bayoumi, *Pure Appl. Chem.* **1965**, *11*, 371.
- [53] B. P. Joshi, J. Park, W. I. Lee, K.-H. Lee, *Talanta* **2009**, *78*, 903.
- [54] C. Grazon, R. C. Baer, U. Kuzmanović, T. Nguyen, M. Chen, M. Zamani, M. Chern, P. Aquino, X. Zhang, S. Lecommandoux, A. Fan, M. Cabodi, C. Klapperich, M. W. Grinstaff, A. M. Dennis, J. E. Galagan, *Nat. Commun.* **2020**, *11*, 1276.
- [55] C. Huang, Y. Qian, *Spectrochim. Acta, Part A* **2019**, *217*, 68.
- [56] Y. Liu, Y. Liu, W. Liu, S. Liang, *Spectrochim. Acta, Part A* **2015**, *137*, 509.
- [57] D. C. Romero, P. Calvo-Gredilla, J. García-Calvo, A. Diez-Varga, J. V. Cuevas, A. Revilla-Cuesta, N. Busto, I. Abajo, G. Aullón, T. Torroba, *Org. Lett.* **2021**, *23*, 8727.